Physical–chemical and catalytic properties of deposited MoO$_3$ and V$_2$O$_5$

**V. Sydorchuk · O. Makota · S. Khalameida ·
L. Bulgakova · J. Skubiszewska-Zięba ·
R. Leboda · V. Zazhigalov**

Abstract The deposition of molybdenum and vanadium oxides onto fumed silica, titania, and alumina as supports through dry milling has been carried out. The structure of prepared compositions has been investigated by means of XRD, DTA–TG, FTIR, and UV–Vis spectroscopy, nitrogen adsorption. The deposited crystal phases are sufficiently uniformly distributed on support surface. The supported oxides are subjected to dispersion in process of milling to the state of oligomeric or isolated species. Milled bulk and deposited MoO$_3$ (first of all, on alumina) possesses improved catalytic performance in process of epoxidation of 1-octene. Vanadium pentoxide also has higher activity in this process.

Keywords Vanadium and molybdenum oxides ·
Deposition · Dry milling · XRD · Epoxidation

Introduction

The epoxidation reaction of unsaturated compounds by hydroperoxides is very important process of chemical industry and organic synthesis [1]. It allows to obtain various valuable oxygen-containing compounds, for example epoxides, which find applications for production of epoxy resins, polymers, surfacelly and biologically active substances, for preparation of pharmaceuticals, etc. Therefore, epoxides are very important industrial products and building blocks in fine organic synthesis. They are still mostly produced via catalytic epoxidation of olefins by different oxidants. However, the use of catalysts in many cases is limited by their cost and difficult preparation. Particularly, the oxide catalyzed epoxidation of unsaturated compounds giving epoxides is an important reaction in organic synthesis. Molybdenum and vanadium compounds, including oxides, using *tert*-butyl hydroperoxide (TBHP) as terminal oxidant are capable to epoxidate olefins [2, 3]. At the same time, MoO$_3$ and V$_2$O$_5$ attract much attention as oxidation catalysts owing to their availability, cheapness and easy of deposition onto the highly dispersed supports [4–7]. Mechanochemical treatment (milling) allows significantly to improve the catalytic performance both of individual MoO$_3$ and V$_2$O$_5$ and their compositions in process of mild oxidation and oxidative dehydrogenation of hydrocarbons [8–11]. It is interesting to study indicated method of catalysts activation for other processes. Therefore, the investigation of milling influence on catalytic properties of bulk and deposited MoO$_3$ and V$_2$O$_5$ in epoxidation reaction is aim of presented work.

V. Sydorchuk (✉) · S. Khalameida · V. Zazhigalov
Institute for Sorption and Problems of Endoecology NAS
of Ukraine, 13 Naumov Str., 03164 Kyiv, Ukraine
e-mail: bilychi@ukr.net

O. Makota · L. Bulgakova
Institute of Chemistry and Chemical Technologies, L'viv
National Polytechnic University, 12 Stepan Bandera Str.,
79013 L'viv, Ukraine

J. Skubiszewska-Zięba · R. Leboda
Faculty of Chemistry, Maria Curie-Sklodowska University,
Maria Curie-Sklodowska Sq. 3, 20-031 Lublin, Poland

Experimental section

Initial reagents

Coarsely dispersed nonporous crystalline V$_2$O$_5$ and MoO$_3$ pushed in Fluka (both analytically pure), possessing specific surface area 6 and 1 m^2 g^{-1}, respectively, were used

in work. Oxides were studied as individual compounds and in the form of composition with the ratio V:Mo = 0.7:0.3.

Fumed silica, titania, alumina (Oriana, Ukraine) with specific surface area 45–346, 64, and 95 $m^2 g^{-1}$, respectively, were utilized as supports for preparation of deposited catalysts. It should be noted that silica and alumina are X-ray amorphous while titania consists of crystal phases of anatase (dominant phase) and rutile. The compositions contain 20% w/w of corresponding oxide on indicated supports.

1-Octene and chlorbenzene (solvent) were also obtained from Aldrich. TBHP was synthesized from *tert*-butyl alcohol and hydrogen peroxide in the presence of sulfuric acid by the procedure given in [12].

Mechanochemical treatment

Mechanochemical treatment (MChT) of indicated individual oxides, their composition with the ratio V:Mo = 0.7:0.3 and mixture with support was carried out using a planetary ball mill of Pulverisette-6 type (Fritsch). Ten balls made of silicon nitride with a 15 mm diameter (total ball mass—130 g) were used. The rotation speed was 600 and 300 rpm at milling of bulk oxides and at deposition onto support, respectively. The duration was 1–6 h and 0.5 h, respectively. The milling media were air ("dry" treatment), 96% ethanol and water at treatment of bulk oxides. The deposition was carried out in air. Therefore, active components (vanadium and molybdenum oxides) were deposited onto surface of supports by means of simultaneous dry milling of vanadium and molybdenum oxides with supports. The milled substance loading was 10 g. The mass ratio of sample and liquid during the treatment was 0.1. Dispersions of oxides milled in water and ethanol were dried at 80 °C.

Study of physical–chemical characteristics

The starting reagents and products of their mechanochemical transformations were studied by means of X-ray powder diffraction (XRD) using a diffractometer Philips PW 1830 with Cu K_α radiation. It should be noted that XRD investigations were performed in identical conditions which was allowed to reveal tendencies in changes of reflexes intensities in row of studied samples. The primary crystallites size D was calculated using the broadening of the most intensive lines according to Sherrer's equation. Curves of DTA and TG were recorded using apparatus Derivatograph-C (F. Paulik, J. Paulik, L. Erdey) in the range of temperature 20–700 °C at the heating rate 10 °C min^{-1}. The DRIFT spectra in the range 4000–400 cm^{-1} were registered using the spectrometer "Spectrum-One" (Perkin-Elmer). The ratio of sample and

KBr powders was 1:20. KBr was dried at 600 °C during 2 h before measurements. Diffuse reflectance UV–Vis spectra of powders were registered on Lambda 35 UV–Vis spectrometer (Labsphere RSA-PE-20 diffuse reflectance and transmittance accessory, Perkin-Elmer Instruments). $BaSO_4$ was used as a reference. Reflectance measurements were converted to absorption spectra using the Kubelka–Munk function.

The adsorption–desorption isotherms of N_2 were measured at 77 K using an automatic gas adsorption analyzer ASAP 2405 N ("Micromeritics Instrument Corp") after outgassing of the samples at 150 °C for 2 h. Volume of mesopores V_{me} and specific surface area S_{BET} were determined from adsorption data.

Epoxidation reaction

The epoxidation reaction was carried out in a thermostated glass reactor equipped with a reflux condenser and a magnetic stirrer under an argon atmosphere at temperature 100 °C during 1 h. Typically, chlorbenzene, TBHP, and 1-octene were charged into the reactor and heated up to the reaction temperature under stirring and then oxide catalyst was added. TBHP was used as the oxidant for this reaction to avoid the necessity of application phase transfer catalyst (co-catalyst) which is necessary in the case of hydrogen peroxide. The introduction of the catalyst was considered as the start of the reaction. The reaction mixture was periodically sampled for analysis. The hydroperoxide concentration was determined by iodometric titration. Other components of reaction mixtures were analyzed by using a Hewlett Packard HP 6890 N chromatograph, a capillary column DB-1 packed with dimethylsiloxane. The column temperature was changed from 50 to 250 °C, with an increment of 10 °C min^{-1}. Concentration of components in reaction mixture was followed: 2.4 mol L^{-1} of 1-octene, 0.4 mol L^{-1} of TBHP, 0.5 g L^{-1} initial bulk catalyst, and 2.5 g L^{-1} supported catalyst.

Results and discussions

XRD, BET, and DTA–TG analysis

The structure of milled molybdenum and vanadium oxides and their composition was analyzed with the help of XRD, DTA–TG, FTIR, and Raman spectroscopy in our previous publication [11]. In summary, observed changes as result of milling are as follows: destruction of crystal structure of oxides and surface reorientation of their main crystallographic planes, increase of imperfectness and formation of new active centers on surface, dispergation of crystal grains and growth of specific surface area. Analogous

investigations are presented in this work for deposited oxides. These results are compared with ones obtained for bulk oxides. Figures 1 and 2 show influence of V$_2$O$_5$ and MoO$_3$ milling in the presence of fumed silica, titania, and alumina as supports on crystal structure of resulted compositions. Diffractograms of prepared compositions based on silica and alumina (which, as mentioned above, are amorphous) contain only lines related to deposited oxides (Fig. 1, curves b, d; Fig. 2, curves b, c). The sample on the base of titania displays reflexes of anatase (these reflexes are marked by symbol °) along reflexes of V$_2$O$_5$ (Fig. 1, curve c) and MoO$_3$ (Fig. 2, curve d). Besides, mechanochemical deposition causes the appearance of sharp background and significant decreasing of intensity of all peaks I_{hkl} for V$_2$O$_5$ as well as MoO$_3$ compared with bulk oxides (Table 1, columns 2 and 4). However, the degree of reduction in intensity is not significant as was observed owing to milling of individual
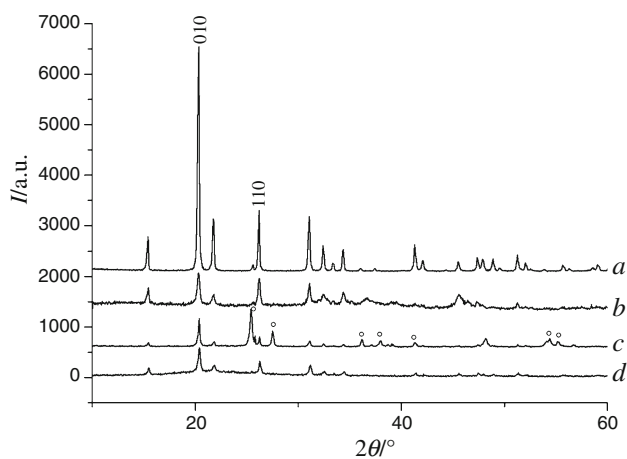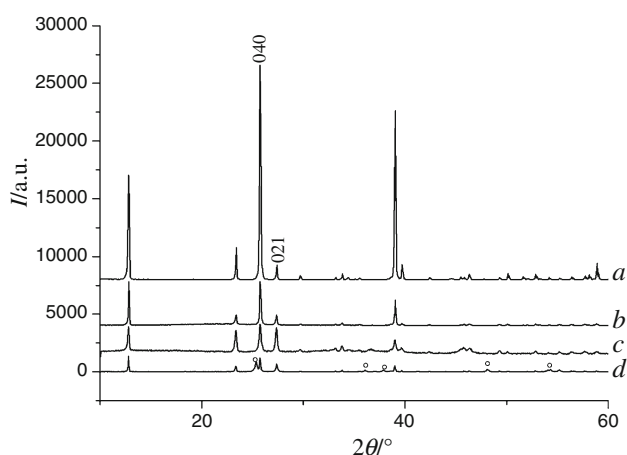
V$_2$O$_5$ and MoO$_3$ [10, 13]. Thus, I_{010} for V$_2$O$_5$ (in terms of its content in the composition) decreases by approximately 1.5 times as a result of deposition onto all supports while this parameter is reduced in 4.5 times after milling of bulk V$_2$O$_5$ in the same conditions [13]. The degree of reduction of I_{040} for MoO$_3$ is larger compared with deposition of V$_2$O$_5$ (but smaller than at milling of individual MoO$_3$) and depends on the nature of the support: I_{040} decreases in 1.3, 1.7 and 3.5 times after MoO$_3$ deposition onto silica, alumina, and titania, respectively. Corresponding decreasing reaches 10 or more times when individual molybdenum trioxide is subjected to dry milling.

The change of ratios between intensities of main reflexes of V$_2$O$_5$ and MoO$_3$ (which are characterized surface orientation of corresponding crystallographic planes) for milled supported compositions also occurs. For example, value of I_{010}/I_{110} for V$_2$O$_5$ (ratio of intensities for reflex from basal plane, containing V=O group, and reflex corresponding to lateral plane) sharply decreases at deposition (i.e., surface content of lateral plane increases) as it is observed after milling of individual V$_2$O$_5$ (Table 1, column 3). At the same time, I_{021}/I_{040} for MoO$_3$, on contrary, increases as a result of deposition onto all supports (column 5). However, reorientation of these planes, which is a consequence of milling of individual MoO$_3$ [10], does not observed.

Therefore, partial dissipation of energy supplied to the system during milling of vanadium and molybdenum oxides in the presence supports takes place. Nevertheless, size of V$_2$O$_5$ and MoO$_3$ crystallites, calculated from broadening of reflexes, decreases to some extent as a result of mechanochemical deposition on supports (Table 1, column 6) although this does not occurs during milling of individual oxides in the same conditions. The latter is associated with parallel realization of dispersion of larger crystallites and the aggregation of smaller ones [14]. Obviously, superfine oxide supports inhibit processes of aggregation of deposited oxides crystallites. On the other hand, particles of supports become larger, which is typical for the milling of highly dispersed materials [14]. As a result, specific surface area of milled compositions reduces (Table 1, column 7). In general, specific surface area S of resulted compositions is determined by value of S for used supports. It is interesting, that S of all supported samples measured via BET method and additive values of S differ by no more than 10%. It should be noted that prepared milled samples are high-dispersed non-porous (loosely packed) powders.

DTA curves for all milled deposited samples contain endoeffects of adsorbed water removal in the range 20–200 °C which are accompanied by mass loss on TG curves. Besides, noticeable mass loss (1–2.5% w/w depending on support kind) is observed above 200 °C. The latter can be related to release of water that strongly bound

Fig. 1 XRD of V$_2$O$_5$: initial (a), deposited on Al$_2$O$_3$ (b), TiO$_2$ (c), A-50 (d)

Fig. 2 XRD of MoO$_3$: initial (a), deposited on A-50 (b), Al$_2$O$_3$ (c), TiO$_2$ (d)

Table 1 Some structural chsracteristics of supported V_2O_5 and MoO_3

Samples	I_{010}/a.u.	I_{010}/I_{110}	I_{040}/a.u.	I_{021}/I_{040}	D/nm	S/m^2 g^{-1}
Initial MoO$_3$	–	–	18,500	0.07	25	1
Bulk MoO$_3$ milled on air	–	–		3.26	25	9
MoO$_3$/TiO$_2$	–	–	1,600	0.58	23	23
MoO$_3$/ A-50	–	–	3,090	0.24	21	44
MoO$_3$/Al$_2$O$_3$	–	–	2,850	0.87	20	52
Initial V$_2$O$_5$	4,450	3.80	–	–	27	6
Bulk V$_2$O$_5$ milled on air		1.23	–	–	26	16
V$_2$O$_5$/TiO$_2$	820	2.90	–	–	25	27
V$_2$O$_5$/A-50	505	2.20	–	–	22	50
V$_2$O$_5$/A-380	535	1.30	–	–	21	187
V$_2$O$_5$/Al$_2$O$_3$	550	1.20	–	–	23	62

to surface defects which are appeared during milling [11, 13].

FTIR spectroscopy

FTIR spectra of milled compositions, prepared on the base of silica and titania, contain only intensive absorption bands (a.b.) which are attributed to support (Figs. 3, 4): with maximum at 1070–1100, 950, 800, 650, 550–580, and 460–475 cm^{-1}. This can be associated with the significant predominance of the support in a composition, as well as the fact that the a.b. of components are overlapped. Indeed, the main a.b. for V_2O_5 are revealed at 1020, 840, 625, and 530 cm^{-1} [9, 15] and for MoO_3 they are observed at 990, 865, 820, 495 cm^{-1} [10, 16]. On the other hand, strong absorption in the range 1200–1000, 800, and 600–400 cm^{-1} is present in spectra of silica and titania [17]. True, maximum of absorption on all spectra is observed at around 820 cm^{-1} which indicates that this band is a superposition of absorption caused deposited oxides and support. At the same time, absorption in the range 1200–1000 cm^{-1} is not characteristic for alumina [17, 18]. Therefore, a.b. 1016 and 996 cm^{-1} related to V_2O_5 and MoO_3, respectively, are clearly revealed on the spectra of compositions based on alumina (Figs. 3, 4 curves a).

UV–Vis spectroscopy

More detailed information about structure of deposited phases was obtained with the help UV–Vis spectroscopy that get a deeper insight on the state of the vanadia and molybdena at support surface [19]. It is known that UV–Vis absorption spectra reflect the electronic structure of valence bands in solids. However, the broad bands in the spectra of metal oxides make it difficult to define the
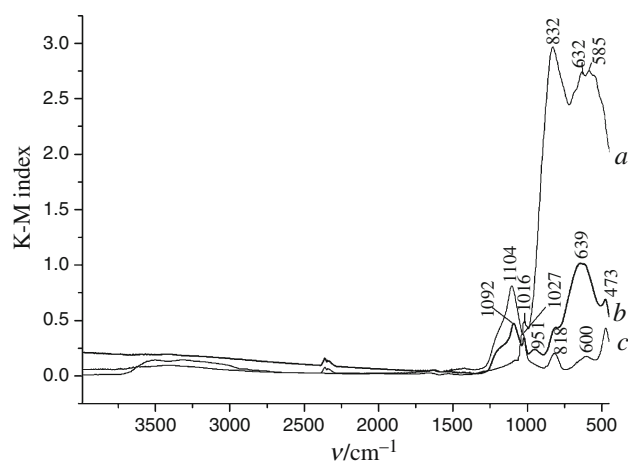

Fig. 3 FTIR spectra of V_2O_5 deposited on: Al$_2$O$_3$ (a), TiO$_2$ (b), A-380 (c)
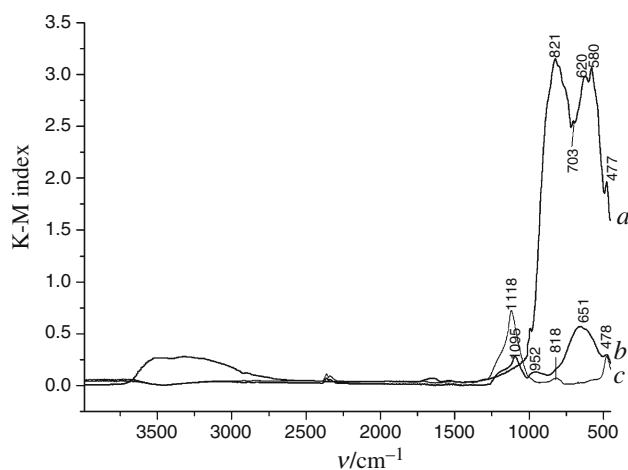

Fig. 4 FTIR spectra of MoO_3 deposited on: Al$_2$O$_3$ (a), TiO$_2$ (b), A-380 (c)

position of these bands from the energy at maximum absorption. At the same time, the absorption edge energies provide a more convenient description of the electronic properties of solids. The information obtained on the band energy gap is particularly useful to evaluate local structure and the dispersion (particle or domain size) of transition metal oxides [19–21]. Thus, it is known that higher energy of charge transfer transition (shorter wavelength) is, the lesser particles size of oxides is. Besides, absorption edge λ (and band gap energy) determined from UV–Vis spectra may serve as a correlating parameter for oxidation–reduction potential of deposited oxides.

In the Table 2 some results calculated from UV–Vis spectra of bulk V_2O_5 and MoO_3 and their mixture are present. The spectrum of pure V_2O_5 contains a.b. with maxima around 475 and 365 nm and exhibits the adsorption edge at 549 nm (Fig. 5, curve a). Indicated bands are attributed to low-energy O^{2-} to V^{5+} charge transfer in highly polymerized vanadium oxide species [20, 22, 23]. The milling causes the shift of band 475 nm to 460, 455, and 410 nm using ethanol, water and air as medium, respectively. Besides, the adsorption edge shifts from 549 to 540, 534 and 538 nm (so-called "blue" shift is observed). UV–Vis spectrum of initial MoO_3 displays the band with maximum around 365 nm and adsorption edge at 428 nm (Fig. 6, curve a) which agrees with results described in [19, 21, 24, 25] for bulk molybdenia. Similarly to vanadia, the milling promotes to shift of these parameters towards low wavelengths (Table 2, column 4). Similar changes are observed in the spectra of mixed compositions.

All these results confirm decrease of crystallite size, as indicated above according to XRD and adsorption data [11].

Mechanochemical deposition of V_2O_5 on supports results in following alterations in the UV–Vis spectra of deposited samples (Fig. 5, curves c–e). As in the case of the bulk vanadia subjected to dry milling, spectra of all supported samples contain intensive band with maximum around 395–400 nm which is assigned to oligomeric species containing fewer V–O–V bonds than bulk V_2O_5 [23]. These spectra also reveal close values of absorption edge,
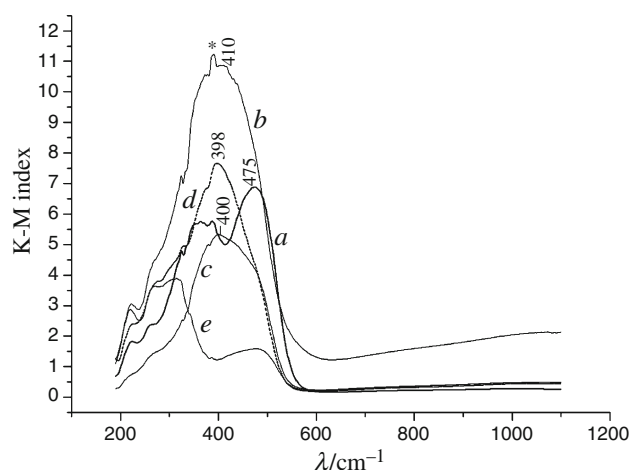

Fig. 5 UV–Vis spectra for V_2O_5: bulk initial (*a*), bulk milled in air (*b*), supported on A-50 (*c*), Al_2O_3 (*d*), TiO_2 (*e*)

Table 2 Some properties of initial and milled bulk MoO_3, V_2O_5 and their mixture

Sample	Medium	S/ m² g⁻¹	λ/ nm	TBHP conversion/%	Epoxide yield[a]/%	$W_{O_2} \times 10^{6b}$/ mol L⁻¹ s⁻¹	$W_{hp} \times 10^{5c}$/ mol L⁻¹ s⁻¹	$W_{ep} \times 10^{5d}$/ mol L⁻¹ s⁻¹
Initial MoO₃	–	1	428	75	47	7	8	13
MoO₃	Air	14	408	82	75	9	3	36
MoO₃	Ethanol	7	413	64	54	14	2	14
MoO₃	Water	6	415	55	43	12	2.5	10
Initial V₂O₅	–	6	549	57	11	35	11	2
V₂O₅	Air	9	538	72	12	45	15	3
V₂O₅	Ethanol	14	540	73	8	42	13	2
V₂O₅	Water	20	534	75	4	59	23	1
Initial V₂O₅/ MoO₃	–	4	549	61	13	25	12	3
V₂O₅/MoO₃	Air	5	581	76	27	30	13	7
V₂O₅/MoO₃	Ethanol	16	537	71	20	47	12.5	5
V₂O₅/MoO₃	Water	10	534	67	16	45	10	3

[a] In account on TBHP hydroperoxide consumption

[b] Initial rate of 1-octene oxidation process by molecular oxygen

[c] Initial rate of TBHP unproductive decomposition in the oxidation reaction of 1-octene by TBHP

[d] Initial rate of TBHP consumption for epoxide formation in the oxidation reaction of 1-octene by TBHP
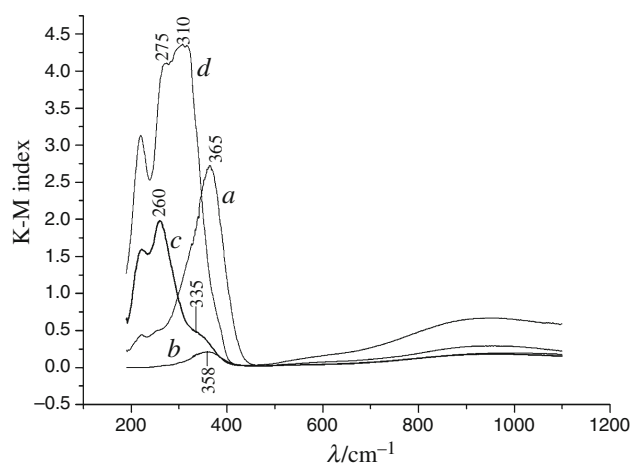
Fig. 6 UV–Vis spectra for MoO₃: bulk initial (*a*), supported on A-50 (*b*), Al₂O₃ (*c*), TiO₂ (*d*)

Table 3 Catalytic properties of supported V_2O_5 and MoO_3

Samples	λ/nm	TBHP conversion/%	Selectivity of 1,2-epoxyoctane formation[a]/%
Initial MoO_3[a]	428	46	66
MoO_3/TiO_2	405	35	64
$MoO_3/$ A-50	425	43	71
MoO_3/Al_2O_3	400	55	83
Initial V_2O_5[a]	549	39	20
V_2O_5/TiO_2	551	44	15
V_2O_5/A-50	543	60	20
V_2O_5/A-380	541	61	23
V_2O_5/Al_2O_3	536	61	21

[a] Catalytic tests for bulk oxides were carried out using content of catalyst in reaction mixture 0.5 g L^{-1}

namely 536–541 nm (Table 3, column 2). The latter is obviously evidence that in the presence of support vanadium pentoxide is subjected to a stronger dispersion compared with milling of bulk sample.

On contrary, deposition of MoO_3 on supports is accompanied by the almost complete disappearance of the band 365 nm (this most clearly seen in the spectrum *c* which is related to the sample prepared on the base of alumina) and a sharp increase in intensity of absorption with maximum at 265–270 nm (Fig. 6). The latter band is also attributed to charge transfer transitions energy O^{2-} to Mo^{6+} [21, 26], namely to isolated molybdenum oxide centers in tetragonal geometry while band at 360 nm accords to octahedral Mo species. Therefore, the degree of MoO_3 dispersion onto supports surface is larger than that observed for V_2O_5. This can be associated with the fact that specific surface area increases more during dry milling of molybdena than vanadia [8, 10, 25].

Epoxidation over bulk oxides

First of all, it was established that in the noncatalytic epoxidation reactions of 1-octene by TBHP is slightly consumed, and respective epoxides are not formed in the reaction mixtures. The catalytic activity of bulk oxides is different and depends on nature of metal as well as medium of milling. Thus, milling of MoO_3 in all media results in increasing of selectivity to epoxide while TBHP conversion increases only for MoO_3 milled in air (Table 2, columns 5, 6). The improvement of selectivity can be associated with significantly enrichment of the surface plane (021), which is responsible for the selective oxidation [10, 27]. Indeed, milling of molybdenum trioxide in all media causes increase of ratio I_{021}/I_{040} [10, 11]. The rise of TBHP conversion is e obviously explained by higher dispersity of sample milled in air which is indirectly confirmed by the UV–Vis spectra. The epoxide yield increases in 1.2–1.25 time (and achieves 75–80%) in comparison with that for initial sample, as a result.

On contrary, milled V_2O_5 exhibits significantly higher TBHP conversion compared with initial sample. At the same time, the selectivity to epoxide reduces after milling of individual vanadia in all media which can be associated with decrease of basal plane (010) content at the surface: ratio I_{010}/I_{110} is lowered in process of milling [11]. Mixed oxides display catalytic performances which are conformed to the rule of additivity.

The initial rate of TBHP consumption for epoxide formation in the oxidation reaction of 1-octene by TBHP W_{ep} increases for all samples milled in air and decreases for samples milled in water (column 9) whereas initial rate of TBHP unproductive decomposition W_{hp} reduces for all milled MoO_3 and V_2O_5 compared with initial samples, but practically is not changed for mixed milled samples (column 8).

It was also established that all samples activate the oxidation reaction only in the presence of TBHP as homogenous initiator when molecular oxygen was added in the initial stages. The highest value of initial rate of 1-octene oxidation process by molecular oxygen W_{O_2} as well as TBHP unproductive decomposition W_{hp} is observed for V_2O_5 milled in water (columns 7, 8). At the same time, the oxidation of 1-octene by TBHP proceeds with the highest initial rate of TBHP consumption for 1,2-epoxyoctane formation W_{ep} (and with minimal W_{hp}) in the presence MoO_3 milled in air. As mentioned above, this sample exhibits also maximal yield of epoxide.

The examples of kinetic curves of TBHP consumption in the presence of vanadia catalysts are presented on Fig. 7. It is seen that the use of milled catalysts noticeable accelerates this process compared with initial (unmilled) sample. It is noteworthy that the course of the kinetic
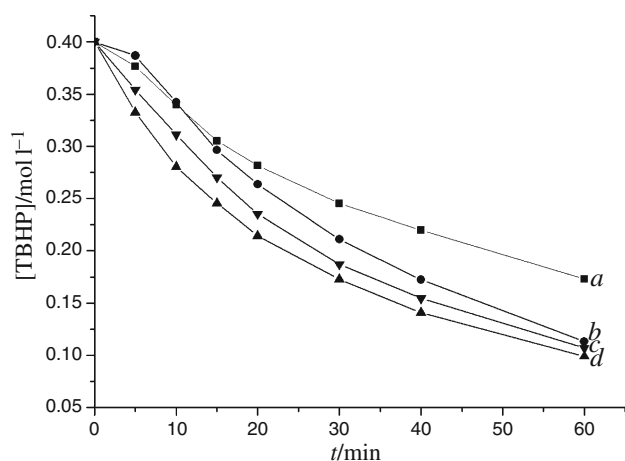
Fig. 7 Kinetic curves of TBHP consumption catalyzed by bulk V$_2$O$_5$: initial (*a*) and milled in air (*b*), ethanol (*c*), water (*d*)

curves little depends on medium of catalysts treatment. This is obviously explained by increasing of dispersity (specific surface area) of catalysts which occurs during their milling.

Epoxidation over supported oxides

The deposition of vanadia and molybdena on oxide supports, possessing high specific surface area, during dry milling also allows to improve the catalytic properties of resulted compositions. Thus, deposition of MoO$_3$ leads to noticeable increase of epoxide formation selectivity compared with bulk MoO$_3$: selectivity has maximal value for composition MoO$_3$/Al$_2$O$_3$. The same catalyst possesses the highest activity: TBHP conversion is 9% higher than that obtained for initial MoO$_3$. The latter is obviously explained the higher dispersity of deposited MoO$_3$ that is confirmed by presence of band centered around 260 nm for composition MoO$_3$/Al$_2$O$_3$ (Fig. 6, curve c). This band corresponds to isolated Mo–O species. As in the case of bulk samples, the gain in selectivity may be associated with an increase in the relative content of plane (021) on surface of supported samples (Table 1, column 5).

On contrary, deposition of V$_2$O$_5$ does not change its low selectivity to epoxide, while activity for compositions V$_2$O$_5$/support sharply increases and exceeds that obtained for compositions MoO$_3$/support. The kinetic curves of TBHP consumption catalyzed by supported V$_2$O$_5$ are similar to those presented above on Fig. 7 for bulk vanadia. As for the bulk catalysts mechanochemical deposition of oxides on supports promotes to accelerate of oxidant consumption. In this case, significant increase in the specific surface area of resulted compositions and maintenance of them in free-dispersed state, obviously, is the cause of observed acceleration.

It should be added that milled bulk and deposited catalysts exhibit stable catalytic performance at least for 5 h, during which the tests were carried out. Besides, milled catalysts were used in three cycles of epoxidation without loss in activity and selectivity.

Conclusions

Dry mechanochemical deposition of molybdenum and vanadium oxides onto supports, possessing high specific surface area, facilitates the dispersion of the active phase which is confirmed by data of XRD and UV–Vis spectroscopy. This is typical, especially, for compositions containing MoO$_3$/Al$_2$O$_3$ for which the formation of isolated Mo–O centrtes are observed. The modification of crystal structure, namely decrease of reflexes intensity and change of ratio for intensities of main peaks, takes place. The resulted compositions are high-dispersed non-porous powders.

The increasing dispersity of active phase as a result of milling can result in the higher activity of deposited compositions. At the same time, rise of selectivity to epoxide formation for bulk and supported MoO$_3$ is associated with increase surface content of plane (021) which is a result of milling. Interaction of MoO$_3$ with basic alumina surface possible also causes improved selectivity of this composition to epoxide formation in comparison with compositions based on low-acid silica and titania.

References

1. Ted Oyama S, editor. Mechanism in homogeneous and heterogeneous epoxidation catalysis. Amsterdam, Elsevier; 2008.
2. da Palma Carreiro E, Burke AJ. Catalytic epoxidation of olefins using MoO$_3$ and TBHP: Mechanistic considerations and the effect of amine additives on the reaction. J Mol Catal A. 2006;249:123–8.
3. Moussa N, Ghorbel A, Grange P. Vanadia-silica catalysts prepared by sol–gel method: application for epoxidation reaction. J Sol-Gel Sci Technol. 2005;33:127–32.
4. Centi G, Cavani F, Trifiro F. Selective oxidation by heterogeneous catalysis. New York: Kluwer/Plenum; 2001.
5. Oyama ST. Crystal face anisotropy of propilene oxidation on molybdenum trioxide. Bull Chem Soc Jpn. 1988;61:2585–94.
6. Bielanski A, Najbar M. V$_2$O$_5$–MoO$_3$ catalysts for benzene oxidation. Appl Catal A. 1997;157:223–61.
7. Dai H, Bell AT, Iglesia E. Effects of molybdena on the catalytic properties of vanadia domains supported on alumina for oxidative dehydrogenation of propane. J Catal. 2004;221:491–9.
8. Zazhigalov VA, Haber J, Stoch J, Kharlamov AI, Bogutskaya LV, Bacherikova IV, Kowal A. Influence of the mechanochemical

treatment on the reactivity of V-containing oxide systems. Solid State Ionics. 1997;101–103:1257–62.

9. Zazhigalov VA, Khalameida SV, Litvin NS, Bacherikova IV, Stoch J, Depero L. Effect of the mechanochemical treatment of a V_2O_5/MoO_3 oxide mixture on its properties. Kinet Catal. 2008; 49:692–701.

10. Bogutskaya LV, Khalameida SV, Zazhigalov VA, Kharlamov AI, Lyashenko LV, Byl' OG. Effect of mechanochemical treatment on the structure and physicochemical properties of MoO_3. Theor Exp Chem. 1999;35:242–6.

11. Skwarek E, Khalameida S, Janusz W, Sydorchuk V, Konovalova N, Zazhigalov V, Skubiszewska-Zięba J, Leboda R. Influence of mechanochemical activation on structure and some properties of mixed vanadium-molybdenum oxides. J Therm Anal Calorim. 2011. doi:10.1007/s10973-011-1744-x.

12. Milas NA, Surgenor DM. Studies in organic peroxides. VIII. *t*-butyl hydroperoxide and *di*-t-butyl peroxide. J Am Chem Soc. 1946;68:205–8.

13. Khalameida S, Skubiszewska-Zięba J, Zazhigalov V, Leboda R, Wieczorek-Cuirowa K. Chemical and phase transformation in the V_2O_5-$(NH_4)_2Mo_2O_7$ system during the mechanochemical treatment in various media. J Therm Anal Calorim. 2010;101:823–32.

14. Heinike G. Tribochemistry. Berlin: Academie Verlag; 1980.

15. Repelin Y, Husson E, Abello L, Lucazeau G. Structural study of gels of V_2O_5: normal coordinate analysis. Spectrochim Acta. 1985;41A:993–1003.

16. Eda K. Longitudinal-transverse splitting effects in IR absorption spectra of MoO_3. J Solid State Chem. 1991;95:64–73.

17. Davydov AA. Molecular spectroscopy of oxide catalyst surfaces. Chichester: Wiley and Sons; 2003.

18. Khaleel AA, Klaubunde KJ. Characterization of aerogel prepared high-surface-area alumina: in situ FTIR study of dehydroxilation and pyridine adsorption. Chem Eur J. 2002;8:3991–8.

19. Herrera JE, Kwak JH, Hu JZ, Wang Y, Peden CHF. Synthes of nanodispersed oxides of vanadium, titanium, molybdenum and tunsten on mesoporous silica using atomic layer deposition. Top Catal. 2006;39:245–55.

20. Khodakov A, Yang J, Su S, Iglesia E, Bell AT. Structure and properties of vanadium oxide–zirconia catalysts for propane oxidative dehydrogenetion. J Catal. 1998;177:343–51.

21. Thielemann JP, Ressler T, Walter A, Tzolova-Muller G, Hess C. Structure of molybdenum oxide supported on silica studied by Raman, UV-Vis and X-ray absorption spectroscopy. Appl Catal A. 2011;399:28–34.

22. Hess C. Direct correlation of the dispersion and structure in vanadium oxide supported on silica SBA-15. J Catal. 2007; 248:120–3.

23. Bulanek R, Capek L, Setnička M, Cičmanec P. DR UV-Vis study of the supported vanadium oxide catalysts. J Phys Chem C. 2011;115:12430–8.

24. Weber RS. Effect of local structure on the UV-visible absorption edges of molybdenum oxide clusters and supported molybdenum oxides. J Catal. 1995;151:470–4.

25. Mestl G, Srinivasan TKK, Knozinger H. Mechanically activated MoO_3. 3. Characterization by vibration spectroscopy. Langmuir. 1995;11:3795–804.

26. Rana RK, Visvanathan B. Mo incorporation in MCM-41 type zeolite. Catal Lett. 1999;52:25–9.

27. Lytvyn NS, Khalameida SV, Zazhigalov VO. Effect of the mechanochemical treatment on properties of MoO_3. Rep Natl Acad Sci Ukraine. 2010;9:108–13 (in Russian).